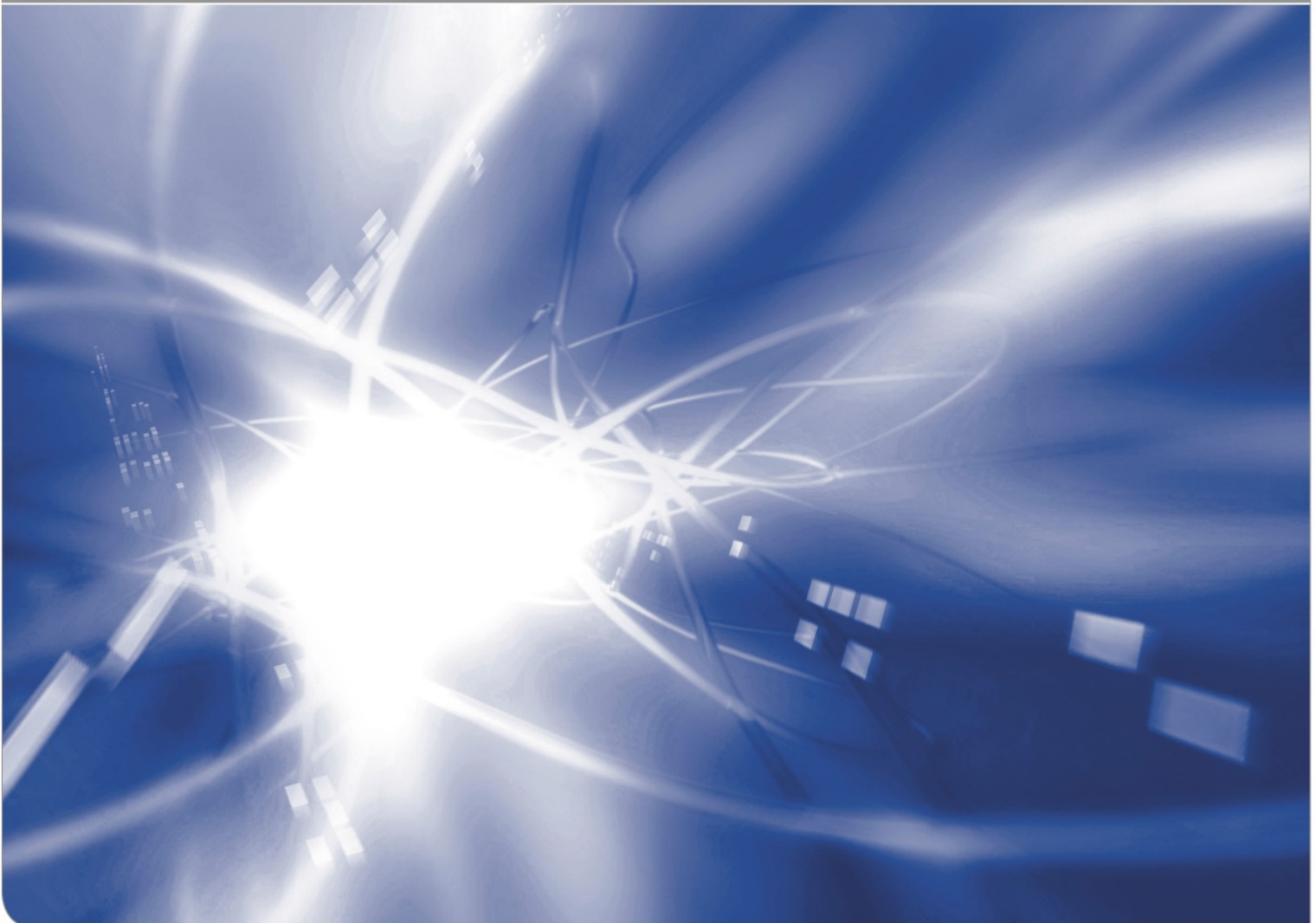


Elimination of swelling stresses from measurements of the equilibrium constant in silica

T. Fett, K. G. Schell

KIT SCIENTIFIC WORKING PAPERS 117



IAM Institute for Applied Materials

Impressum

Karlsruher Institut für Technologie (KIT)
www.kit.edu



This document is licensed under the Creative Commons Attribution – Share Alike 4.0 International License (CC BY-SA 4.0): <https://creativecommons.org/licenses/by-sa/4.0/deed.en>

2019

ISSN: 2194-1629

Abstract

The reaction of water with silica is described by the equilibrium constant k . This property depends on temperature and is affected by stresses. The experimental determination of k is in most cases carried out in presence of swelling stresses. Knowledge of the reaction volume $\Delta\bar{V}$ allows an elimination of the swelling stresses and the determination of an equilibrium constant for the case of a stress-free material. An analytical expression of k_0 as a function of temperature, $k_0=f(T)$, will be suggested.

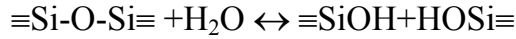
Contents

1	Hydroxyl concentration under water saturation pressure	1
1.1	Results from literature	1
1.2	Computation of molecular and hydroxyl water concentrations	2
1.3	Semi-logarithmic description	4
2	Influence of swelling stress	5
3	Equilibrium constant in the absence of any stress	6
4	Application of the equilibrium constants	7
	References	8

1 Hydroxyl concentration under water saturation pressure

1.1 Results from literature

Water in silica reacts with the silica network according to



with the concentration of the immobile hydroxyl $[\equiv\text{SiOH}] = S$ and that of the mobile molecular water $[\text{H}_2\text{O}] = C$, [1]. Hydroxyl concentrations at silica surfaces below 500°C are available from investigations by Tomozawa and co-workers [2,3,4] and Zouine et al. [5]. The results from Zouine et al. [5] are shown in Fig. 1. The saturation pressures p , under which the tests were carried out, are represented in Fig. 1a. For these measurements the *nuclear reaction analysis* (NRA) was applied that subsumes molecular and hydroxyl water.

Whereas in [2-4] the S -concentration was measured via the IR-method, the data by Zouine et al. [5] represent the total water content C_w at the surface. The results are shown in Fig. 1b. From these measurements, also the water species S and C can be obtained.

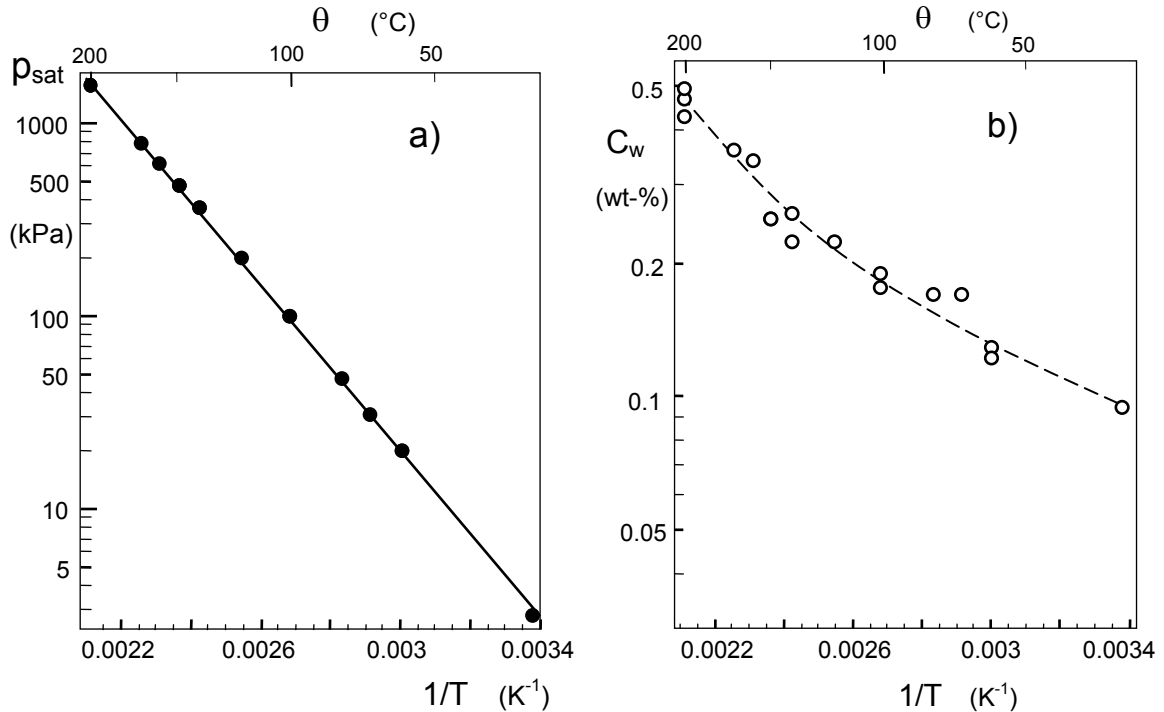


Fig. 1 Results by Zouine et al. [5], a) saturation pressure with symbols indicating the test conditions, b) solubility of water at silica surfaces under saturation pressure.

1.2 Computation of molecular and hydroxyl water concentrations

In *molar units*, the total water concentration is given by

$$C_w = C + \frac{1}{2}S = C(1 + \frac{1}{2}k) \quad (1.1)$$

where the quantity k is the equilibrium constant describing the ratio of $k=S/C$.

The experimental results on equilibrium ratios from literature were expressed in [6] for the temperature range of $90^\circ\text{C} \leq T \leq 350^\circ\text{C}$ by the empirical relation

$$k = \frac{S}{C} \cong A_s \exp\left(-\frac{Q_s}{RT}\right) \quad (1.2)$$

($A_s=32.3$ and $Q_s=10.75$ kJ/mol, subscript “s” for saturation pressure) as is shown by the straight line in Fig. 2 together with the 95%-confidence limits of the straight-line fit as the dashed curves.

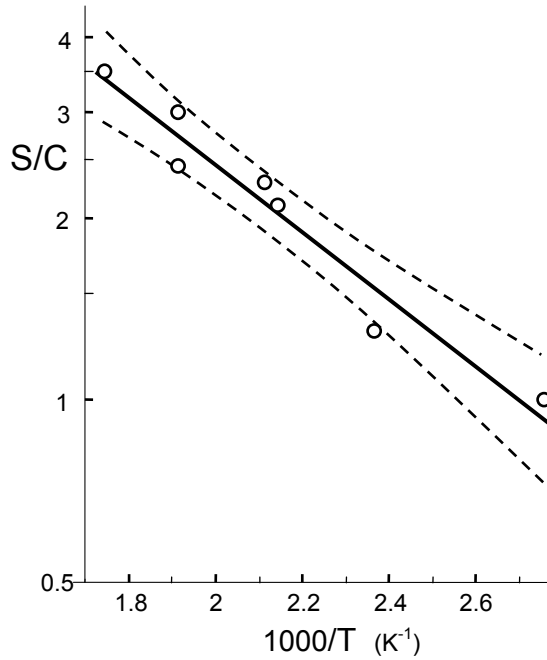


Fig. 2 Plot of $k=S/C$ as a function of $1/T$, from [6].

Equations (1.1) and (1.2) result in

$$C = \frac{C_w}{1 + \frac{1}{2}k}, \quad (1.3)$$

$$S = \frac{C_w}{\left(\frac{1}{2} + \frac{1}{k}\right)} \quad (1.4)$$

and in *mass units*

$$S = \frac{17}{18} \frac{C_w}{\left(\frac{1}{2} + \frac{1}{k}\right)} \quad (1.4a)$$

(the ratio 17/18 reflects the different mole masses of water and hydroxyl). For the temperature range of $20^\circ\text{C} \leq \theta \leq 200^\circ\text{C}$, the straight-line dependency can be approximated as

$$p_{\text{sat}} \cong B_1 \exp\left(-\frac{B_2}{RT}\right) \quad (1.5)$$

($B_1=5.79 \times 10^7$ kPa, $B_2=41.28$ kJ/mol).

Under the common assumption that the molecular water species at the surface is proportional to the pressure of the water vapour, $C \propto p/T$, the combination with the two $1/T$ -dependencies for k and p makes clear that the total water concentration at the surface, eq.(1.1) not necessarily shows a straight line in an Arrhenius plot. This behaviour is visible from the dashed curve in Fig. 1b.

The concentrations of molecular and hydroxyl water were computed from the measured total water concentration by using eq.(1.3) and (1.4a) and are plotted in Fig. 3 versus $1/T$. The dashed curves are guidelines for the eyes.

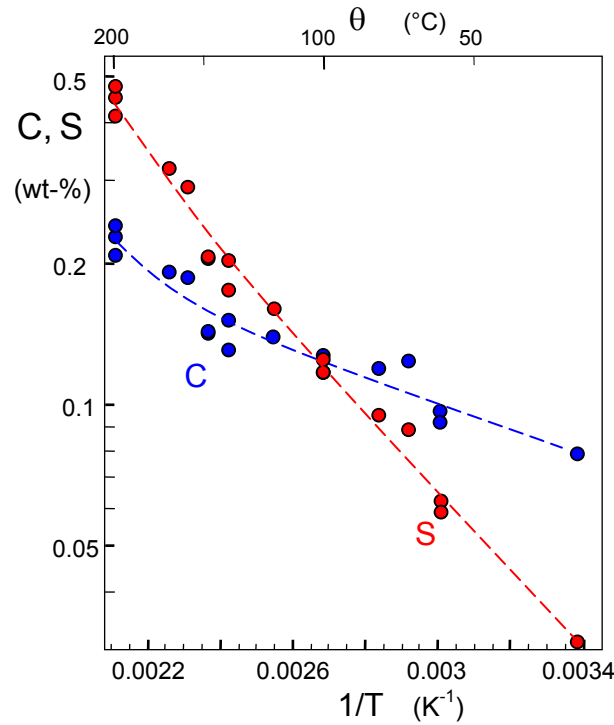


Fig. 3 Surface concentration of the molecular (blue) and hydroxyl (red) water species obtained via eqs.(1.3), (1.4a).

1.3 Semi-logarithmic description

Figure 4a shows the total water concentration in a semi-logarithmic plot with linear temperature scaling. The measurements can approximately be described by the simple expression

$$C_w = 0.000780 \exp(0.00868 \theta) \quad \text{for } 23^\circ\text{C} \leq \theta \leq 200^\circ\text{C} \quad (1.6)$$

with the temperature θ in $^\circ\text{C}$. Fig. 4b illustrates the S -data in a similar plot with a slightly curved averaging curve given by

$$S = \frac{17}{18} \frac{0.000780 \exp(0.00868 \theta)}{\frac{1}{2} + \frac{1}{A_s} \exp(Q_s / RT)} \quad (1.7)$$

with the parameters A and Q in eq.(1.2).

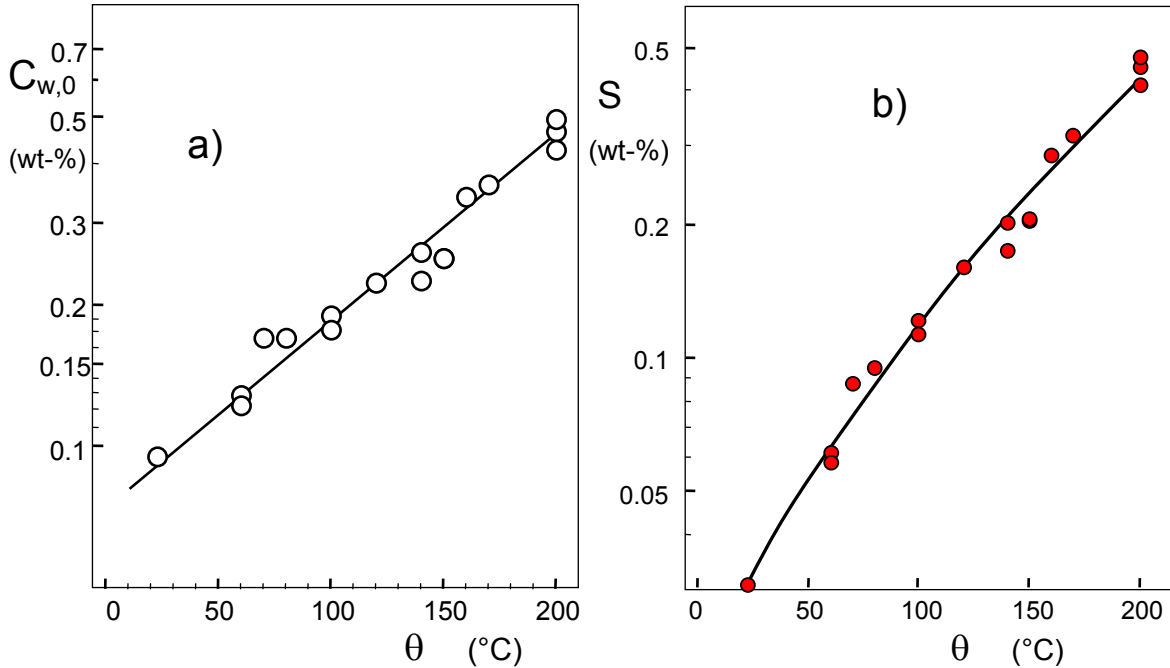


Fig. 4 a) Total water from Fig. 1b and hydroxyl data of Fig. 3 plotted with linear abscissa scaling, b) hydroxyl water concentration, curve: eq.(1.7) obtained by combining eqs.(1.6) and (1.2).

For simple computations in the reduced temperature range of $70^\circ\text{C} \leq \theta \leq 200^\circ\text{C}$, tolerating a few percentage deviations from the curve in Fig. 4b, a straight-line representation is suggested that reads

$$S_{\text{sat}} \approx 0.000265 \exp(0.0143 \theta) \quad \text{for } 70^\circ\text{C} \leq \theta \leq 200^\circ\text{C} \quad (1.7a)$$

This approximation is introduced in Fig. 5 as the red line. For extrapolations, the eq.(1.7a) should not be used. Already at $\theta=250^\circ\text{C}$, the hydroxyl concentration is over-estimated by about 30%.

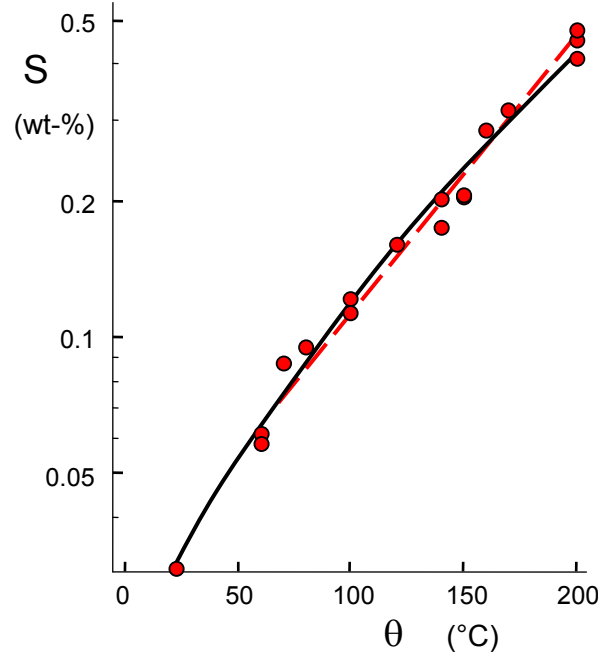


Fig. 5 Hydroxyl data of Fig. 4b together with the simple straight-line approximation by eq.(1.7a).

2 Influence of swelling stress

The swelling stresses at the glass surfaces are given by

$$\sigma_{sw,z} = \sigma_{sw,y} = -\kappa \frac{E}{3(1-\nu)} S \cong -28 \text{ GPa} \times S \quad (2.1)$$

with the hydrostatic stress

$$\sigma_{sw,h} = \frac{1}{3}(\sigma_{sw,z} + \sigma_{sw,y}) = -18.7 \text{ GPa} \times S \quad (2.2)$$

For the computation of the swelling stresses, the necessary hydroxyl concentration can be determined via eq.(1.4a) with the equilibrium constant according to eq.(1.2). Introducing the hydroxyl concentrations from eq.(1.7) results in the swelling stresses

$$\sigma_{sw,h} = \frac{13.75 \text{ MPa} \exp(0.00868 \theta)}{\frac{1}{2} + \frac{1}{A} \exp(Q/RT)} \quad (2.3)$$

represented by the curve in Fig. 6a.

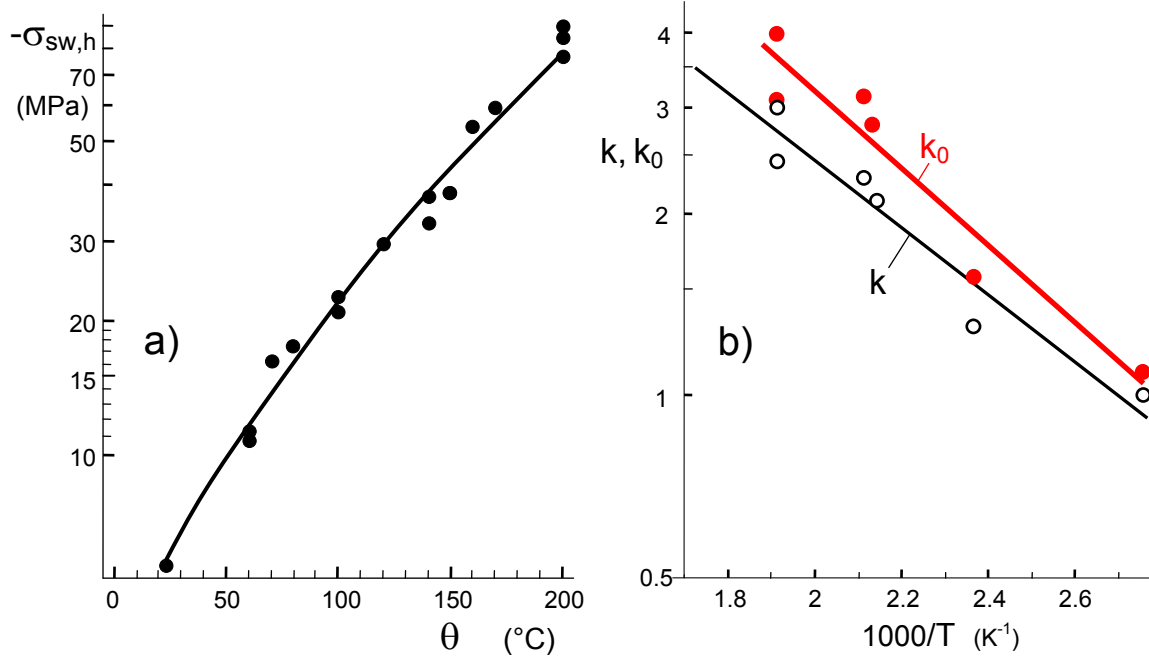


Fig. 6 a) Hydrostatic swelling stresses under saturation water pressure, b) equilibrium constant for disappearing swelling stresses, k_0 , as a function of $1/T$ shown by the red straight line and the closed circles, obtained via eqs.(3.1) and (3.2). Black curve and open circles: values of k from measurements under saturation water vapor pressure (from Fig. 2).

3 Equilibrium constant in the absence of any stress

The equilibrium constant of the water/silica reaction is given by

$$\frac{k}{k_0} = \exp\left[\frac{\sigma_h \Delta \bar{V}}{RT}\right] \quad (3.1)$$

where k_0 is the equilibrium constant in the absence of any stress, namely externally applied stresses and swelling stresses, $\Delta \bar{V}$ is the reaction volume, the change in the volume of the glass during the chemical reaction, *i.e.*, the volume of the products minus the volume of the reactants during the reaction. R is the universal gas constant and T is the temperature in K . The reaction volume was found in [7] as

$$\Delta \bar{V} = 2\bar{V}_s = 15.03 \text{ cm}^3/\text{mole} [14.22, 15.8] \quad (3.2)$$

with the 95%-CI in brackets.

By using eq.(2.3), the data k_s for the specimens for saturated water vapour pressure were transformed in k_0 via eqs.(3.1) and (3.2). The resulting data points are represented by the red circles in Fig. 6b. They were fitted by an Arrhenius dependency according to

$$k_0 = A_0 \exp\left(-\frac{Q_0}{RT}\right) \quad (3.3)$$

($A_0=58.9$ and $Q_0=12.14$ kJ/mol with subscripts “0” for disappearing swelling stresses) as is shown by the red line in Fig. 6b. The black line and the open circles show again the equilibrium constants from Fig. 2 for saturation pressure.

A short remark seems to be necessary with respect to the meaning of the measured equilibrium constants. In the preceding equations, the measured values of the equilibrium constant were interpreted as values representing all the water present at and below the glass surface. It has to be noted that in the region below the surface the water concentrations decrease with the distance to the surface. This implies that the swelling stresses and the equilibrium constant must also vary with depth z .

The value k is mostly obtained in literature by transmission IR measurements of hydroxyl and molecular water. These measurements reflect average values \bar{k} over the whole water profiles

$$\bar{k} = \frac{\bar{S}}{\bar{C}} = \frac{\int S(z)dz}{\int C(z)dz} \quad (3.4)$$

Having this in mind, eq.(1.2) has to be understood as

$$\bar{k} = \frac{\bar{S}}{\bar{C}} = A \exp\left(-\frac{Q}{RT}\right) \quad (3.5)$$

4 Application of the equilibrium constants

In order to eliminate the effect of increasing surface concentrations with increasing saturation pressure, Fig. 1a, the concentrations were normalized on the pressure of 355 Torr. In contrast to Fig. 3, the surface concentrations decrease with increasing temperature. This makes clear that the increasing curves of Fig. 1b and Fig. 3 reflect strongly the increasing saturation pressure.

The data in Fig. 7a, transformed via eq.(1.2) and describing concentrations of molecular water and hydroxyl in the absence of externally applied stresses, can be represented by straight lines for $1/T > 0.0022/\text{K}$:

$$C_{355 \text{ Torr}} \cong \exp\left[-23.58 + \frac{35.84 \text{ kJ/mol}}{RT}\right] \quad (4.1)$$

and

$$S(0)_{355 \text{ Torr}} \cong \exp\left[-20.16 + \frac{25.09 \text{ kJ/mol}}{RT}\right] \quad (4.2)$$

In order to show the effect of the swelling stress on the hydroxyl concentration, we computed again the S -concentration for a pressure of 355 Torr by application of eq.(3.3) and introduced the results as the solid red circles in Fig. 7b. Since 355 Tor is

the saturation pressure at 80°C, the data below this temperature (black circles) are without physical relevance. The open circles represent measurements were reported by Davis and Tomozawa [3]. Whereas the hydroxyl concentration decreases with increasing temperature for temperatures $\theta < 250^\circ\text{C}$, it increases for $\theta > 250^\circ\text{C}$.

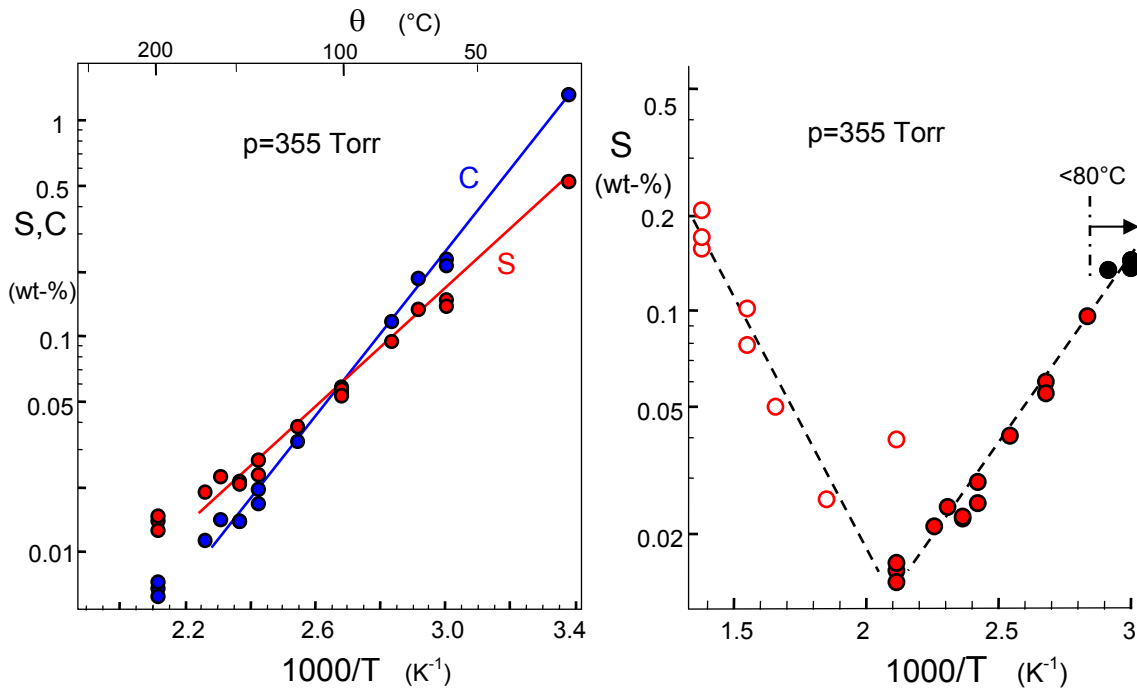


Fig. 7 a) Concentrations of molecular and hydroxyl water from Fig. 3, normalized on a constant water vapour pressure of $p = 355$ Torr, b) data by Zouine et al. [5] transformed from saturation pressure to 355 Torr via eq.(3.3) (solid red circles) and results reported by Davis and Tomozawa [3] (open circles).

References

- 1 Doremus, R.H., Diffusion of water in silica glass, *J. Mater. Res.* **10**(1995), 2379-89.
- 2 Wakabayashi, H., Tomozawa, M., Diffusion of water into silica glass at low temperature, *J. Am. Ceram. Soc.* **72**(1989), 1850-55.
- 3 Davis, K.M., Tomozawa, M., Water diffusion into silica glass: structural changes in silica glass and their effect on water solubility and diffusivity, *J. Non-Cryst. Sol.* **185** (1995), 203-220.
- 4 Oehler, A., Tomozawa, M., Water diffusion into silica glass at a low temperature under high water vapor pressure, *J. Non-Cryst. Sol.* **347**(2004) 211-219.
- 5 A. Zouine, O. Dersch, G. Walter and F. Rauch, "Diffusivity and solubility of water in silica glass in the temperature range 23-200°C," *Phys. Chem. Glass: Eur. J. Glass Sci and Tech. Pt. B*, **48** [2] 85-91 (2007).

6 S. M. Wiederhorn, F. Yi, D. LaVan, T. Fett, M.J. Hoffmann, Volume Expansion caused by Water Penetration into Silica Glass, *J. Am. Ceram. Soc.* **98** (2015), 78-87.

7 T. Fett, K.G. Schell, S.M. Wiederhorn, Swelling strains from gamma-irradiated silica - Evaluation of results by Shelby, *Scientific Working Papers* **103**, 2018, ISSN: 2194-1629, Karlsruhe, KIT.

KIT Scientific Working Papers
ISSN 2194-1629

www.kit.edu